Veterinary Microbiology 236 (2019) 108376

Contents lists available at ScienceDirect

Veterinary Microbiology

journal homepage: www.elsevier.com/locate/vetmic

Taishan *Pinus Massoniana* pollen polysaccharide inhibits the replication of acute tumorigenic ALV-J and its associated tumor growth

Qiuju Wang[a,1], Yongqiang Miao[a,1], Yulin Xu[a], Xiuyan Meng[b], Wenping Cui[a], Yujian Wang[a], Lin Zhu[a], Zhou Sha[a], Kai Wei[a,*], Ruiliang Zhu[a,*]

[a] College of Animal Science and Technology, Shandong Agricultural University, Taian, Shandong, 271000, China
[b] Taishan Polytechnic, Taian, Shandong, 271000, China

ARTICLE INFO

Keywords:
Avian leukosis virus
Taishan *Pinus Massoniana*pollen polysaccharide
RNA-Seq
Signaling pathway
Antiviral
Antitumor

ABSTRACT

Avian leukosis virus subgroup J (ALV-J) has resulted in considerable economic losses in the poultry industry. In recent years, fibrosarcoma induced by ALV-J, which contains the v-fps oncogene, has gained momentum, and this has brought about new challenges to the poultry industry. To study the inhibitory effects of Taishan *Pinus Massoniana* pollen polysaccharide (TPPPS) on acute ALV-J infection and tumor development, antiviral and antitumor models of the Fu-J (SDAU1005) strain of ALV-J were established *in vitro* and *in vivo*. The results of *in vitro* experiments showed that TPPPS significantly inhibited viral replication in a dose-dependent manner during adsorption and pretreatment stages. The results of *in vivo* experiments have shown that TPPPS significantly reduced the viral load in the plasma and tumor tissues, as well as inhibited tumor growth. We further examined the difference in transcriptome expression by using RNA-Seq technology. A total of 560 differentially expressed genes were identified that included 329 up-regulated genes and 231 down-regulated genes. The up-regulated genes were mainly immune-related genes, whereas the down-regulated genes were mainly tumor-regulated genes. Gene Ontology (GO) term enrichment included immune system processes, positive regulation of immune system processes, regulation of immune system processes, leukocyte activation, cell activation, and protein binding. Kyoto Encyclopedia of Genes and Genomes (KEGG) pathway analysis revealed that the main immune and tumor-related pathways included T-cell receptor signaling pathway, cytokine-cytokine receptor interactions, natural killer cell-mediated cytotoxicity, PI3K-Akt signaling pathway, JAK-STAT signaling pathway, NF-κB signaling pathway, and Ras signaling pathway. In summary, our results preliminarily point to the antiviral and antitumor mechanism of TPPPS *in vivo* and *in vitro*.

1. Introduction

Avian leukosis virus subgroup J (ALV-J), an alpha retroviral carcinogenic retrovirus, can infect broilers, laying hens, quails, ducks, turkeys, and other poultry (Payne and Nair, 2012; Plachy et al., 2017). Since its identification in chickens in 1991, ALV-J has spread rapidly, causing huge economic losses in the poultry industry, especially in China (Gao et al., 2010; Payne and Nair, 2012). ALV-J not only suppresses the immune system, but also causes various types of benign and malignant tumors in commercial laying hens and local chickens (Cheng et al., 2010). Because of its complex gene sequence and antigenic variability, there are no effective measures in place to control its infection. In addition to the chronic and oncogenic form of ALV-J, Chinese investigators have recently isolated an acute and transformed form of ALV-J carrying the v-fps oncogene from fibrosarcoma (Wang et al., 2016). The spread of ALV-J is now threating the poultry industry in China, and new methods of disease control are urgently needed.

Several studies have reported that antiviral drugs can inhibit viral replication. As important macromolecules, plant and animal polysaccharides have highly complex structures and antiviral, antitumor, immunoregulatory, anti-inflammatory, and antioxidative properties (Chen et al., 2016; Kouakou et al., 2013). Polysaccharides have been widely used in the prevention and treatment of human and animal diseases. Taishan *pine Massoniana* pollen polysaccharide (TPPPS) is extracted from the Taishan pine pollen. Its main components are mannose, ribose, xylose, glucuronic acid, galactic acid, glucose, galactose, and arabinose (Yang et al., 2015). Previous studies have shown that TPPPS can enhance subunit vaccine effectiveness and inhibit

* Corresponding authors.
E-mail addresses: zhurl@sdau.edu.cn (R. Zhu), weikaisdau@163.com (K. Wei).
[1] These authors have contributed equally to this work

https://doi.org/10.1016/j.vetmic.2019.07.028
Received 26 April 2019; Received in revised form 29 July 2019; Accepted 29 July 2019

infection of immunosuppressive viruses, such as ALV and REV in poultry (Li et al., 2015; Yu et al., 2017). However, the effects of TPPPS on acute tumorigenic ALV-J and its related tumors are still unclear.

Here, we used the Fu-J (SDAU1005) viral stock carrying the v-fps oncogene, an acute tumorigenic ALV-J strain, to investigate the inhibitory effects of TPPPS on the replication of ALV-J and growth of its associated tumor, and to preliminary elucidate the regulatory mechanism. We found that TPPPS could inhibit Fu-J and SDAU1005 viral proliferation in DF-1 cells. In addition, we established an animal model to show that TPPPS could inhibit the replication of the Fu-J (SDAU1005) and reduce the growth of tumors. Combined with RNA sequencing (RNA-Seq), genes that were regulated by TPPPS were identified. Different regulatory genes including in cellular pathways, biological processes, molecular functions, and proteins were identified and analyzed. The reliability of the transcriptome results was verified by quantitative reverse transcription polymerase chain reaction (qRT-PCR). In summary, the regulatory mechanism was preliminary revealed through the above studies.

2. Materials and methods

2.1. Cells, viruses, and reagents

DF-1 cells were cultured in Dulbecco's Modified Eagle Medium (DMEM; GIBCO, Shanghai, China) containing 10% fetal bovine serum in a humidified atmosphere of 5% CO_2 at 37 °C. The Fu-J (SDAU1005) viral stock, which was prepared from the cell-free filtrate of acute fibrosarcomas, could induce fibrosarcomas in chickens rapidly (within 2 weeks) but only gave rise to a mild transformation in cultured CEF. It consisted of both the replication-defective Fu-J(isolated from an ALV-associated acute fibrosarcoma of natural cases in crossbreed broilers) carrying the v-fps oncogen and the ALV-J viral strain SDAU1005 which was the helper virus of Fu-J (Wang et al., 2015). The ALV-J rabbit polyclonal anti-gp85 antibody was kindly gifted from Cheng Ziqiang. The mouse polyclonal anti-fps antibody and TPPPS (whole polysaccharide) was prepared in our laboratory.

2.2. Anti-viral activity of TPPPS in DF-1 cells

DF-1 cells were plated in 6-well plates and pretreated with 50, 100, or 200 μg/mL TPPPS in DMEM. Subsequently, DF-1 cells were infected with the Fu-J (SDAU1005) (10^3TCID$_{50}$ of SDAU1005) and TPPPS at different concentrations. After infection for 2 h, the medium was replaced with DMEM containing different concentrations of TPPPS, and the cells were cultured for 7 days. To quantify the ALV p27 antigen by ELISA kit (IDEXX, Beijing, China), the medium was collected daily. To quantify the Fu-J (SDAU1005) copy number by qRT-PCR, RNA was isolated from cells culture supernatants at 7 days post-inoculation (dpi).

To pinpoint the stage of viral infection, DF-1 cells were plated in 6-well plates and infected with the Fu-J (SDAU1005) (10^3 TCID$_{50}$ of SDAU1005). The cells were then treated with TPPPS at a concentration of 100 μg/mL in five groups as follows:

Pretreatment (Pret): The Fu-J (SDAU1005) were pre-incubated with TPPPS for 1 h at 4 °C and subsequently used for infection. The DF-1 cells were infected with the Fu-J (SDAU1005) and TPPPS for 2 h at 37 °C. After the supernatant was removed, the cells were washed 3 times and recovered in DMEM containing TPPPS.

Adsorption (Ad): The cells were infected with the Fu-J (SDAU1005) and treated with TPPPS for 2 h at 37 °C. After the supernatant was removed, the cells were washed 3 times and recovered in DMEM.

After adsorption (AA): The cells were infected with the Fu-J (SDAU1005) in the absence of TPPPS. After viral adsorption for 2 h at 37 °C, the viruses were removed. The cells were washed 3 times and subsequently incubated with DMEM containing TPPPS.

Always (Al): The cells were infected with the Fu-J (SDAU1005) containing TPPPS. After incubation for 2 h at 37 °C, the supernatants were removed. The cells were washed 3 times and recovered in DMEM containing TPPPS.

Iniorder to quantify Fu-J and SDAU1005 viral copy numbers by qRT-PCR, RNA was isolated. To identify the infected cells by an indirect immunofluorescence assay (IFA), the cells were stained with anti-gp85 and anti-fps antibodies at dpi. The DF-1 cells infected with the Fu-J (SDAU1005) in the absence of TPPPS served as the control.

2.3. In vivo experiments

A total of ninety 1-day-old specific pathogen-free (SPF) chickens were randomly assigned to three sterilized isolators, with each isolator representing an experimental group as follows: V-PBS, V-TPPPS, and PBS. The chickens in the V-TPPPS group received 5.0 mg of TPPPS orally for 7 consecutive days before challenge. The chickens in V-PBS and PBS groups received PBS. Subsequently, the 7-day-old chickens in V-TPPPS and V-PBS groups were subcutaneously challenged with the Fu-J (SDAU1005) (10^4 TCID$_{50}$ of SDAU1005). The chickens in the PBS group were injected with an equivalent volume of PBS. Tumor development and progression were monitored after challenge, and the tumor size and death rate were recorded daily. At 5, 10, 15, and 20 dpi, tumor tissues from chickens in V-PBS and V-TPPPS groups and leg muscles from chickens in the PBS group were collected. The samples were frozen in liquid nitrogen and stored until use. To determine the viral load, total RNA was isolated from the plasma and tumor tissues of chickens in the three groups, and the viral load was determined by qRT-PCR. The lesions caused by viral infection were analyzed by hematoxylin and eosin (H&E) staining.

2.4. High throughput sequencing and analysis

2.4.1. Library construction and RNA-Seq

At 10 dpi, tumors were excised from chickens in V-PBS and V-TPPPS groups. The samples were processed for Illumina deep sequencing. Total RNA was isolated from the samples using the RNA Extraction Kit (Tiangen Biotech Co, Beijing, China). For RNA-Seq, two cDNA libraries (corresponding to V-TPPPS and V-PBS groups) were prepared using the Truseq RNA Sample Prep Kit from Illumina (New England Biolabs, Ipswich, MA, USA). In brief, mRNA was isolated from total RNA using magnetic oligo (dT) beads, and the mRNA was digested into fragments of 200–300 bp. Thereafter, the first- and second-strand cDNA was synthesized, and then PCR-amplified to generate the cDNA library. The cDNA library was sequenced using the Illumina X Ten System at the Shanghai Personal Biotechnology Co., Ltd.

2.4.2. Analysis of high throughput sequencing results

Transcriptome assembly and annotation protocols (Nanjing Personal Biotechnology Co., Ltd., China) were followed. After discarding low quality sequence reads (i.e., reads with adaptors, undefined nucleotides > 5% or Q30 < 10%) with Perl Script, the clean reads were aligned to the gallus reference genome (Gallus-5.0; http://www.ensembl.org/index.html) using Tophat2 Software. The gene expression levels were calculated using reads per kilobase million (RPKM) values generated by Cutadapt Software. Genes (RPKM > 0.1) expressed in all samples were defined as expressed genes. The differentially expressed genes (DEGs) were analyzed using the DESeq R Package. The genes with fold changes ≥ 1.5 and *P*-values < 0.05 were defined as DEGs. The false discovery rate (FDR) was used to evaluate the *p*-value in multiple tests. All DEGs were subjected to Gene Ontology (GO) term enrichment and Kyoto Encyclopedia of Genes and Genomes (KEGG, https://www.kegg.jp/kegg/kegg2.html) pathway analysis. To annotate the functions of the DEGs, GO analysis was performed using TopGO Software.

Table 1
Primers used in this study.

Primer name	Gene sequence(5'-3')	Application gene	Size of fragment
gp85	5'-AACCAATCATGGACGATGGTA-3'	gp85-F	255bp
	'TCCAAAGGTAAACCCATATGC-3'	gp85-R	
fps	5'-GCGAGGGGAACGGACTAATT-3'	v-fps-F	326bp
	5'-CACGCTGTGACATCCACTTCTT-3'	v-fps-R	
GAPDH	5'-GAAGCTTACTGGAATGGCTTTCC-3'	GAPDH-F	200bp
	5'-GGCAGGTCAGGTCAACAACAG-3'	GAPDH-R	
PRF1	5'- ATGGCGCAGGTGACAGTGA -3'	PRF1-F	126bp
	5'- TGGCCTGCACCGGTAATTC -3'	PRF1-R	
CCL5	5'- CTGCCCCAGAATCATGTGAA -3'	CCL5-F	125bp
	5'- CAGCTCCAGGAAGTTGATGTA -3'	CCL5-R	
GZMA	5'- TGGGTGTTAACAGCTGCTCATTGC -3'	GZMA-F	134bp
	5'- CACCTGAATCCCCTCGACATGAGT -3'	GZMA-R	
BCL11B	5'- CCCAGCGGGAAGTTCATC -3'	BCL11B-F	168bp
	5'- AAGTCACGACATCCCAACAGC -3'	BCL11B-R	
HSPA2	5'- CCACCATTCCCACCAAACAA -3'	HSPA2-F	107bp
	5'- ATACACCTGGACGAGGACAC -3'	HSPA2-R	
BAG3	5'- ACCACAACAGCCGAACCA -3'	BAG3-F	112bp
	5'- GATGGGCCATTTGCTGATGAC -3'	BAG3-R	
DNAJA4	5'- AAGTACCACCCCGACAAGAA -3'	DNAJA4	185bp
	5'- TTGGGTCCGACAGAACTTCA -3'	DNAJA4	
HSP90AA1	5'- ACACATGCCAACCGCATTTA -3'	HSP90AA1	195bp
	5'- CCTCCTCAGCAGCAGTATCA -3'	HSP90AA1	

2.5. RNA extraction and qRT-PCR

To measure the mRNA levels of the *v-fps* oncogene and the *gp85* gene, qRT-PCR was carried out. Total RNA was isolated from DF-1 cells, plasma, and tumor tissues with TRIzol (Takara Biotechnology, Dalian, China), according to the manufacturer's instructions. The quantity and quality of the isolated RNA were determined with an Eppendorf BioPhotometer at UV260/280 nm (Hamburg, Germany). Total RNA was transcribed into first-strand cDNA using the PrimeScript RT MasterMix (Takara Biotechnology), according to the manufacturer's instructions. The primers (Table 1) were synthesized by Shanghai Sangon Company (Shanghai, China). Thereafter, the viral loads in DF-1 cells, plasma, and tumor tissues were determined. The expression levels of the DEGs in tumors were measured by qRT-PCR. The results were normalized using GAPDH as the reference gene. The gene expression data were analyzed using the $2^{-\triangle\triangle CT}$ method.

2.6. Statistical analysis

SPSS 17.0 software was used for statistical evaluation, and data were expressed as mean ± SD. qRT-PCR data were analyzed using one-way one-way ANOVA with a Bonferroni post hoc test. *P*-values < 0.05 were considered significant. Statistical comparisons were made using Student's *t*-test. For RNA-Seq data, the expression of genes with ≥ 1.5-fold change and FDR-adjusted P-value < 0.05 were considered significantly different.

3. Results

3.1. TPPPS inhibits the replication of Fu-J and SDAU1005 viruses in DF-1 cells

We investigated the inhibitory effects of TPPPS on the replication of Fu-J and its helper virus SDAU1005 in DF-1 cells by two separate approaches. These assay included ALV-p27 expression levels in cell culture supernatants by ELSA kit (Fig. 1A), and the viral genomic RNA level in cell culture supernatants by qRT-PCR (Fig. 1B). The results showed that TPPPS could inhibit the replication of both Fu-J and SDAU1005 in DF-1 cells in a dose-dependent manner at concentrations from 50 to 200 μg/mL. The optimal inhibitory concentration was 200 μg/ml, but it's not significantly different from 100 μg/ml.

To define the stage at which TPPPS inhibited the replication of Fu-J and SDAU1005, DF-1 cells were treated with 100 μg/mL of TPPPS. The results of qRT-PCR showed that the viral copy number was lower in Pret, Ad, and Al groups than that in the control group at 7 dpi ($P < 0.05$). Although TPPPS showed inhibitory effect in the AA group compared with the control group, the difference was not significant ($P > 0.05$). The Fu-J viral load in the Pret, Ad, and Al groups was significantly lower than that in AA and control groups at 7 dpi, and the inhibitory effect of the Fu-J was higher than that of the SADU1005 (Figs. 1C and 1D). The results of IFA showed that there were fewer Fu-J and SADU1005 in DF-1 cells of Pret, Ad, and Al groups compared to AA and control groups (Fig. 1E).

3.2. TPPPS inhibits the growth of virus-induced fibrosarcoma in vivo

Tumor lesions were assessed in chickens of V-PBS and V-TPPPS groups at 5, 10, 15, and 20 dpi. All chickens of the V-PBS group had tumors by 12 dpi, whereas all chickens in the V-TPPPS group had tumors by 16 dpi (Fig. S1A). Cross-sections of tumors stained with hematoxylin and eosin showed that the tumor cells in V-TPPPS group were significantly lower than that in V-PBS group (Fig. S1B). The median survival for chickens in V-PBS, V-TPPPS, and PBS groups were 19, 24, and 30 d, and the mortality rates were 100%, 60%, and 0%, respectively (Fig. S1C).

3.3. TPPPS inhibits the replication of Fu-J and SDAU1005 viruses

The results of qRT-PCR showed that the viral load in plasma and tumors of chickens in the V-TPPPS group was significantly lower at 5, 10, 15, and 20 dpi than that in the V-PBS group. Although the inhibitory effect of TPPPS was weaker at later stages, the viral load was lower ($P < 0.05$; Figs. 2A and 2B). Furthermore, TPPPS had a moderate inhibitory effect on Fu-J, that may have been caused by the different inhibitory mechanisms of Fu-J and SDAU1005.

3.4. Overview of the mRNA sequencing data

3.4.1. TPPPS modulates the RNA-seq

To understand the regulatory mechanism of TPPPS, we performed transcriptome analysis and compared the expression profiles across groups on a genome-wide scale. Approximately 90.9 giga bases (Gb) of reads were obtained from the six RNA-Seq libraries. After discarding the low-quality reads, a high percentage (range, 72.31–82.96%) of the

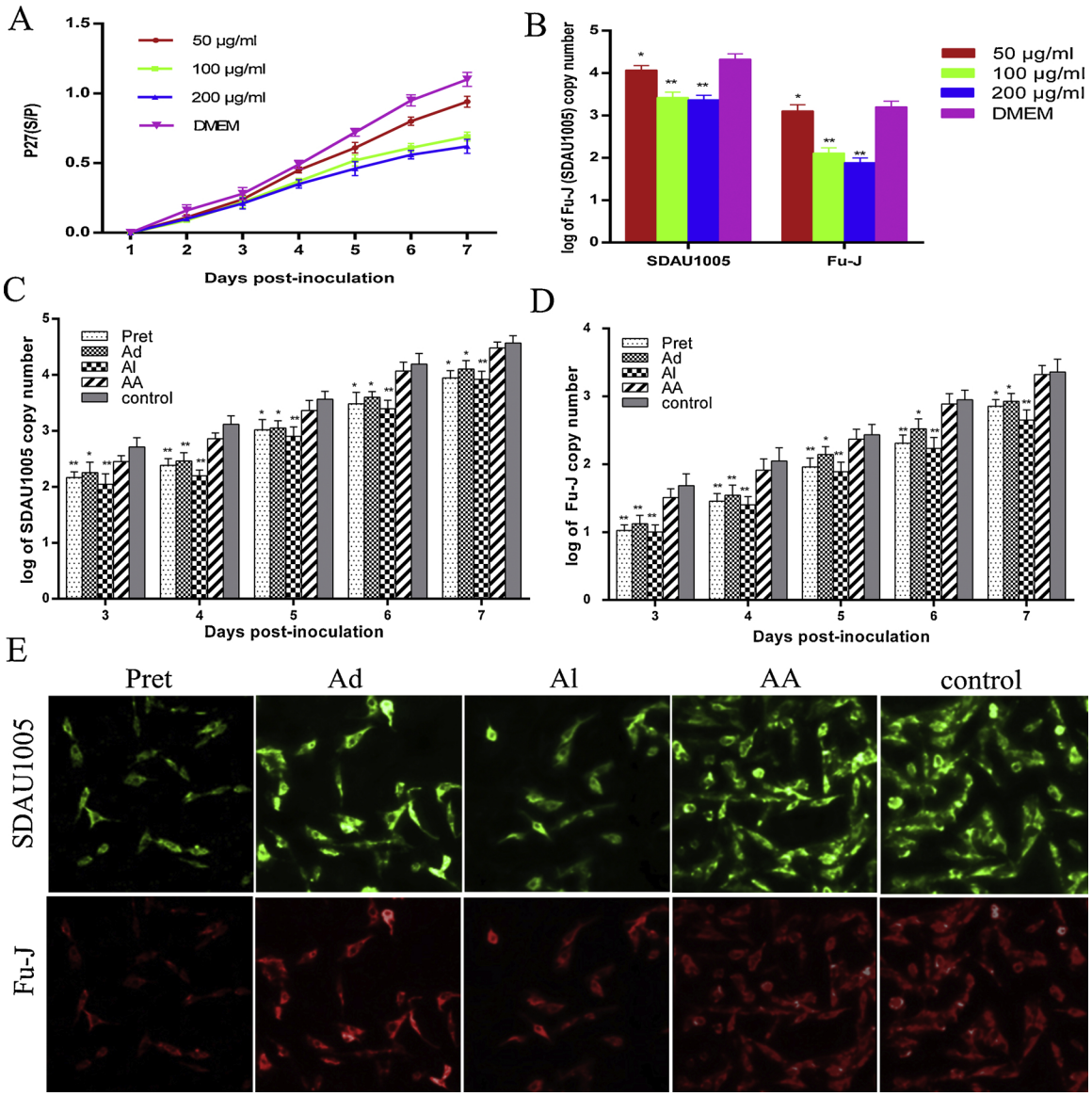

Fig. 1. Inhibitory effects of TPPPS on replication of Fu-J and its helper virus SDAU1005 in DF-1 cells. (A) Comparisons of ALV p27 antigen levels in cell culture supernatants by ELASA at 7 dpi. The cut-off value of positive criteria was 0.2, the vertical axis represents the S/P values in ELISA. (B) Comparisons of expression levels of Fu-J and SDAU1005 in DF-1 cells after treated with different concentration of TPPPS using qRT-PCR. The qRT-PCR data was performed by using the $2^{-\triangle\triangle CT}$ method. Differences in the expression level were assessed by Student's *t*-tests. (C and D) Comparisons of expression levels of Fu-J and SDAU1005 in DF-1 cells treated with 100 μg/mL of TPPPS at different viral infection phases using qRT-PCR, respectively: pretreated (Pret); adsorption phase (Ad); after adsorption (AA); always during the entire infection process (Al); absence of TPPPS in the entire assay (control). (E) IFA detection the expression levels of Fu-J and SDAU1005 in DF-1 cells after treated with TPPPS at 7 dpi. All values shown are expressed as means ± SD of three independent experiments. Differences were considered significant when $P \leq 0.05$ (*) and highly significant when $P \leq 0.01$ (**). The data was representative of the results of three independent experiments.

reads were mapped to the gallus reference genome. Among the mapped reads, 96.97–97.35% were mapped uniquely to the gallus reference genome. Approximately 90% of the reads from the six samples equaled or exceeded the Q30 (Table 2). Pairwise correlations were used to evaluate the individual variations in the tumor samples. Spearman's correlation was high across all genes (range, 0.91–1.00; Table 3). Furthermore, Cuffdiff software was used to quantify the gene expression levels with RPKM, a *P*-value < 0.05, and a fold change (FC) ≥1.5 as the thresholds. Five hundred-sixty genes were differentially expressed in chickens of the V-TPPPS and V-PBS groups. There were 329 (58.75%) of up-regulated DEGs in the V-TPPPS group, whereas 231 (41.25%) of the DEGs were down-regulated in V-PBS group. The heatmap of the DEGs is shown in Fig. S2A, and the expression of each gene was normalized to achieve a standard normal distribution (Fig. S2B). The results of the RNA-Seq analysis were deposited into the NCBI BioProject Database, with accession number PRJNA507309.

3.4.2. Functional categorization of DEGs

GO term enrichment and KEGG pathway analysis were carried out to define the biological significance of the 560 DEGs. Firstly, we investigated the enrichment of the GO categories of the up- and down-regulated genes. Thirty significantly enriched GO terms were identified, including biological processes, cellular components, and molecular functions (Fig. 3). For biological processes, the enriched GO terms were immune system processes, response to stimuli, cellular response to stimuli, positive regulation of response to stimuli, positive regulation of immune system processes, cell communication, regulation of immune system processes, signaling, leukocyte activation, and cell activation. For cellular components, the enriched GO terms were T-cell receptor complexes and chaperonin-containing T-complexes. For molecular

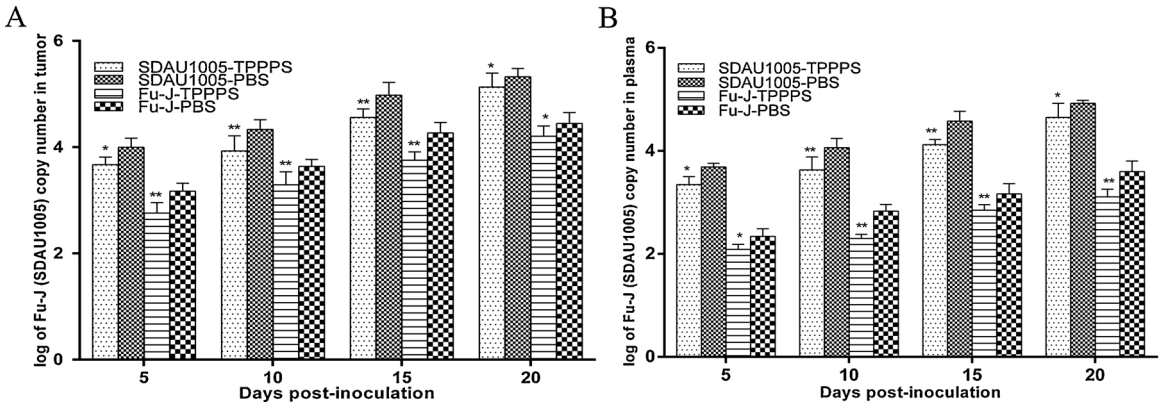

Fig. 2. Effects of TPPPS on replication of Fu-J (SDAU1005) in chickens. (A) Fu-J and SDAU1005 viral load in tumors determined by qRT-PCR demonstrated that TPPPS could inhibit the replication of Fu-J and SDAU1005 in chickens. (B) Fu-J and SDAU1005 viral load in plasma determined by qRT-PCR demonstrated that the replication of Fu-J and SDAU1005 viruses in plasma were also inhibited. The qRT-PCR data was performed by using the $2^{-\triangle\triangle CT}$ method, and differences in the expression levels were assessed by Student's *t*-tests. Differences were considered significant when $P \leq 0.05$ (*) and highly significant $P \leq 0.01$ (**). The data was representative of three independent experiments.

Table 2
Biology repeat correlation statistics.

Sample	sample	r2
A1	A2	0.95
A1	A3	1.00
A2	A3	0.93
B1	B2	0.93
B1	B3	0.91
B2	B3	0.98

functions, the enriched GO terms were unfolded protein binding, chaperone binding, and protein binding. All terms were significantly enriched in biological processes compared to cellular components and molecular functions. Secondly, we performed KEGG pathway analysis and identified several pathways and processes, including cytokine-cytokine receptor interactions, natural killer cell mediated cytotoxicity, chemokine signaling, protein processing in the endoplasmic reticulum, MAPK, estrogen, PI3K-Akt, and Ras signaling. The major pathways are shown in Fig. 4 and Table S1.

3.4.3. Analysis of DEGs associated with immunomodulatory and anti-tumor activity

The mRNA levels of most immune-relevant DEGs, including *MZB1* (15.08 fold increase), *PRF1* (8.43 fold increase), *CCL5* (5.68 fold increase), *CD28* (3.92 fold increase), *CD8A* (3.56 fold increase), and *GZMA* (3.35 fold increase) were higher in the V-TPPPS group than those in the V-PBS group. Information of the immune-relevant DEGs is shown in Table S2.

The expression of tumor-suppressing genes was higher in the V-TPPPS group than that in the V-PBS group. These up-regulated genes included *RASAL1* (10.36 fold increase), *SLURP1* (8.60 fold increase), *GLIPR1* (5.45 fold increase), *PTPN7* (3.29 fold increase), and *CYFIP2* (3.26 fold increase). Compared with the V-PBS group, tumor-causing genes, such as *HSPB9* (0.03 fold increase), *HSPA2* (0.03 fold increase), *BAG3* (0.05 fold increase), *OLFM4* (0.06 fold increase), *DNAJB1* (0.07 fold increase), *FOXJ1* (0.08 fold increase), and *HSP90AA1* (0.22 fold increase) in V-TPPPS group were down-regulated. Information of the anti-tumor DEGs is shown in Table S3.

3.4.4. Validation of RNA-Seq data by qRT-PCR

To validate the results of the RNA-Seq analysis, qRT-PCR was performed. Eight genes, namely *PRF1*, *CCL5*, *GZMA*, *BCL11B*, *HSPA2*, *BAG3*, *DNAJA4*, and *HSP90AA1* were selected and used for qRT-PCR (Table 1). The qRT-PCR results of the eight genes were consistent with those of the RNA-Seq analysis (Fig. S3), indicating that the RNA-Seq data was accurate and reliable.

4. Discussion

The prevalence and spread of the acute tumorigenic ALV-J is a new threat to the poultry industry in China. Polysaccharides are macromolecules with antitumor and antiviral properties. Previous studies in our laboratory have shown that TPPPS could inhibit viral replication by binding to virus particles to block the adsorption of ALV-J. However, it is not clear whether TPPPS exhibit cross-inhibition on acute tumorigenic ALV-J. In this study, both in vitro and in vivo experiments showed that TPPPS significantly inhibited viral replication, reduced viral load at different stages of infection, and inhibited the growth of tumor caused by Fu (SDAU1005). To explain this phenomenon, RNA-Seq was used to further analyze the inhibition of TPPPS on the replication of Fu-J (SDAU1005) and the tumor growth at gene and protein levels.

Tumors affect both humans and animals alike. Avian tumors are mainly caused by viruses, such as ALV and Marek's disease virus. The prevention and treatment of viral-causing tumors should first involve measures that control the viral load. There was a positive correlation between the tumor growth rate and the viral load and the tumor growth could be regulated by controlling the viral number. Astragalus

Table 3
The sequence reads alignment to gallus genome.

Sample	Total reads	Total base pairs	Mapped reads	Uniqely mapped reads	%≥Q30(%)	Mapped to Exon
A1	42583866	6339810308	34150757(80.20%)	33138309(97.04%)	90.86	26235397(92.19%)
A2	44832146	6669603280	35200921(78.52%)	34133898(96.97%)	92.54	25803165(90.53%)
A3	46063146	6860623498	36072010(78.31%)	35026894(97.10%)	92.03	26431788(90.41%)
B1	47035694	6981609308	37209671(79.11%)	36143901(97.14%)	92.53	27563132(91.23%)
B2	45208800	6723600130	36238907(80.16%)	35277151(97.35%)	92.42	27172337(92.23%)
B3	41766812	6221233370	34651350(82.96%)	33587086(96.93%)	93.01	25485084(92.08%)

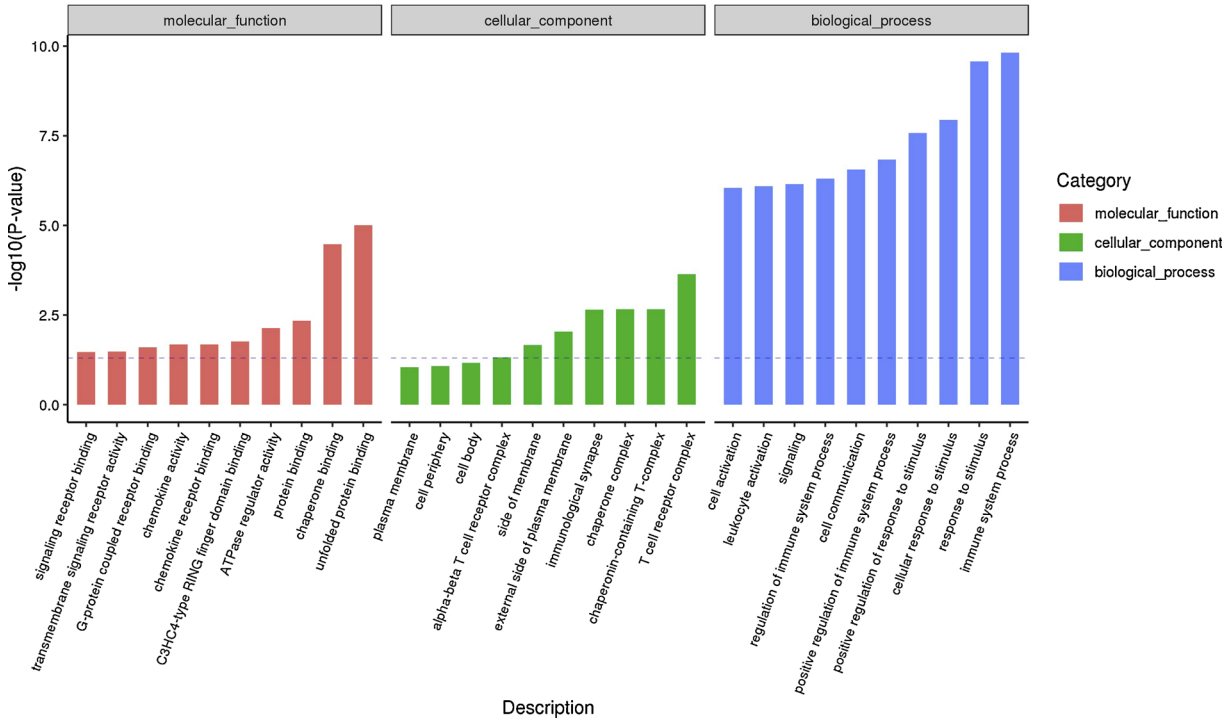

Fig. 3. GO analysis of DEGs between the V-PBS and V-TPPPS groups. The DEGs were classified into three categories: cellular component, molecular function, and biological process.

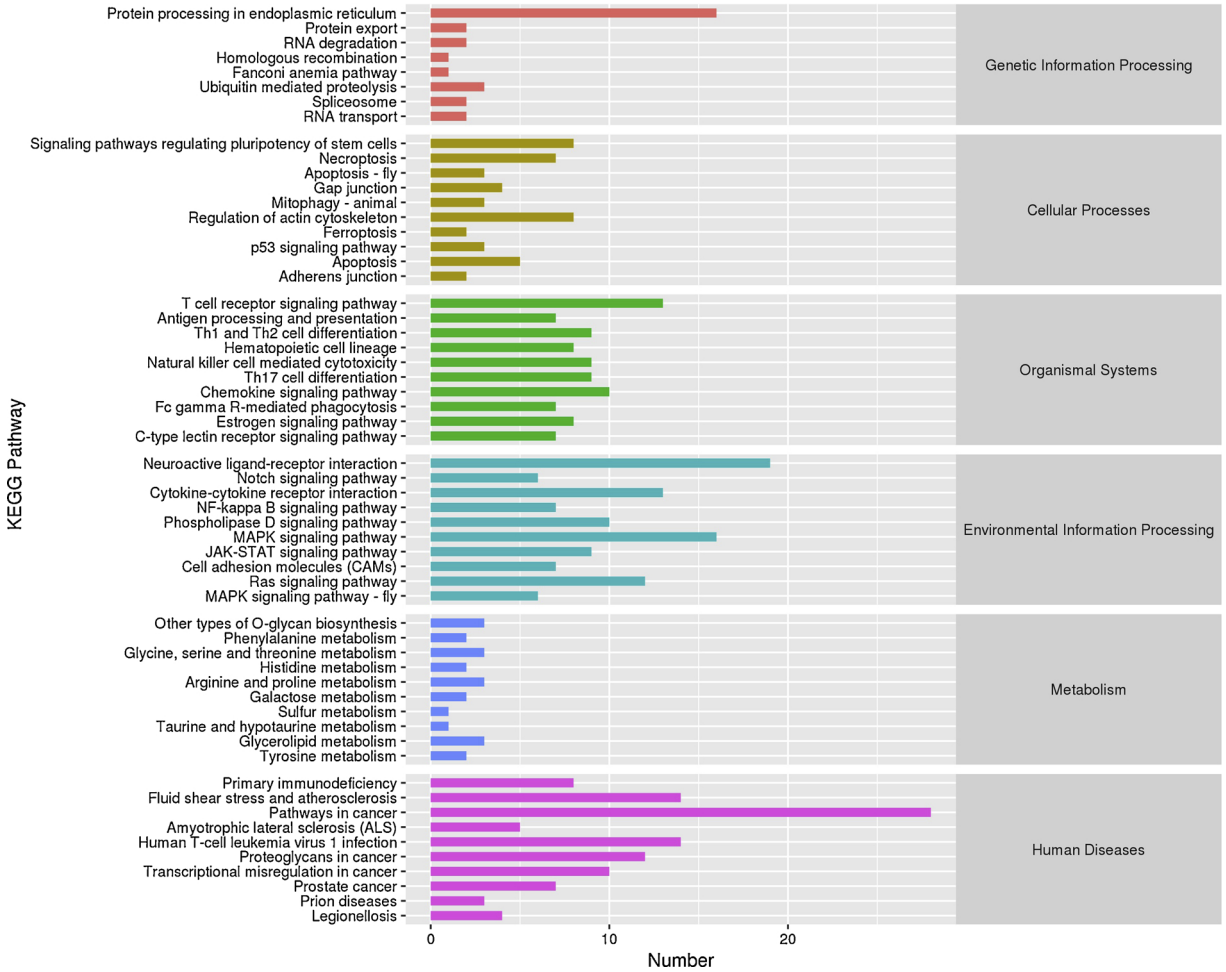

Fig. 4. KEGG analysis of DEGs between the V-PBS and V-TPPPS groups. The number of genes in each category are shown above.

polysaccharide (APS) could significantly reduce the hepatitis B virus (HBV) DNA level in transgenic mice (Dang et al., 2009). In this study, our results showed that TPPPS could inhibit the replication of Fu-J (SDAU1005) and reduce the expression levels of Fu-J and SDAU1005 in plasma and tumors. The antiviral and antitumor effects of TPPPS may involve activation of the immune system, which can have an inhibitory effects on tumors caused by viruses.

Pattern recognition is the first step of innate immunity. Pattern recognition receptors (PRRs) sense the presence of infection and activate immune responses. Studies have shown that only TLR2, TLR4, and TLR3 can bind glycosyl ligands on polysaccharides to activate signal transduction (Chavarria-Velazquez et al., 2018; Huik et al., 2013). APS promoted the proliferation of B lymphocytes and the production of antibodies by binding to the TLR2/4 receptor on the B lymphocyte surface (Zhou et al., 2017). *Radix isatidis* polysaccharides can bind to the TLR3 receptor and activate signaling pathways to inhibit influenza viral replication (Li et al., 2017). The C-type lectin receptor has been reported to be a polysaccharide receptor and could enhance the immune response (Wang et al., 2018). The results of RNA-Seq showed that the mRNA levels of TLR2, TLR3, TLR4, and C-type lectin receptors in the V-TPPPS group were significantly higher than those of the V-PBS group, suggesting that TPPPS regulates these receptor expression. TLR3 functions as a receptor for TPPPS and the virus, indicating that TPPPS can inhibit viral replication by competing with the receptor of virus. However, further studies are needed to understand the mechanisms of the binding of polysaccharides to receptors and the activation of signaling pathways.

The congenital immune system (composed of macrophages, dendritic cells and natural killer cells) and the adaptive immune system (composed of B cells, $CD8^+$ and $CD4^+$ T cells) can inhibit the proliferation of viruses and prevent cancer (Meng et al., 2016). Among the 560 DEGs, most of immune-related genes were up-regulated, as shown in Appendix 1. *PRF1*, *GZMM*, *GZMA*, *CD28*, *CD8B*, *BCL11B*, *CD8A*, *CD3E*, and *CD3D* are mainly involved in cellular immunity. PRF1, CCL5, GZMA and BCL11B are important immune-related T and B lymphocyte secretory proteins (Monteiro et al., 2007). CD3 is a differentiation antigen specifically expressed by mature T cells. $CD4^+$ and $CD8^+$ T are two very important T lymphocyte in adaptive immunity. In addition, CD28 molecules have also been found to stimulate eosinophils to release of IL-2, IL-4, IL-13 and IFN-γ (Rohr et al., 2016). The results showed that white blood cells and lymphocytes played an important role in ALV-J infection. In addition to cellular immunity, humoral immunity plays an important role in antiviral. Immunosuppression was caused by ALV-J infection, which made it difficult for the host to produce antibodies against ALV-J and other antigens. Previous studies showed that TPPPS increased the NDV antibody titer in chickens. RNA-Seq analysis showed that the expression levels of antibody genes, such as MZB1, JCHAIN, IgH, IGLL1, IKZF3, and LRRC8A, in the V-TPPPS group were significantly higher than that in V-PBS group. These results suggested that TPPPS inhibited ALV-J by increasing the titers of the antibodies in V-TPPPS group. Cytokines and their corresponding cytokine receptors constitute key regulators of immune activity. We found that cytokines, such as IRF4, IL21R, IL2RB, STAT4, CCL5, XCL1, CCL4, and CCL7, participating in inflammatory and acquired immune responses were up-regulated. These cytokines were mainly involved in immune and inflammatory responses of chickens, and they may play an important role in antiviral and anti-infection.

Tumorigenesis is a complex process caused by many factors. Viruses induce tumors through multiple oncogenes in their genomes (Justice et al., 2015). As shown in Table 6, 55 major tumor-related genes were identified. The major up-regulated tumor-suppressor genes were *RASAL1*, *SLURP1*, *GLIPR1*, *PTPN7*, and *CYFIP2*. The major down-regulated tumor genes were *HSPB9*, *HSPA2*, *BAG3*, *OLFM4*, *DNAJB1*, *FOXJ1*, and HSP90AA1. Exogenous expression of RASAL1 may inhibit the proliferation and invasion ability of HepG2 cells (Meng et al., 2017). Studies proved that mutations of the SLURP1 gene could cause cutaneous tumors (Bergqvist et al., 2018). GLIPR1 regulates lung cancer growth through the V-Erb-B avian erythroblastic leukemia viral oncogene homolog 3 (ErbB3) (Sheng et al., 2016). PTPN7 is negatively correlated with tumour formation and growth (Meeusen and Janssens, 2018). CYFIP2 knockdown confers resistance to 5-FU-based chemotherapy in gastric cancer cells (Jiao et al., 2017). Secreted BAG3 can induce the release of factors that sustain tumour growth and the metastatic process (De Marco et al., 2018). OLFM4 expression is correlated with cancer differentiation, stage, metastasis, and prognosis in a variety of cancer (Liu and Rodgers, 2016). FOXJ1 expression supports the ependymal differentiation of papillary tumor of the pineal region (Coy et al., 2017). These up-regulated tumor suppressor and down-regulated tumor genes may be the key regulatory genes in the inhibitory effects of TPPPS on tumor growth.

In addition, we also found that the expression of heat stress proteins (HSPs), including *HSPB9*, *HSPA2*, *DNAJB1,* and HSP90AA1, in the V-PBS group were increased. HSPs are not only involved in eliminating heat stress, but also in antigen presentation, protein processing, tumor growth regulation, and antiviral activities (Jhaveri et al., 2012). The elevated HSPs expression indicates that the viral load in the V-PBS group was higher than that in the V-TPPPS group. Viruses can enter chickens to stimulate the production of additional tumor-related genes and promote tumor growth, which was also the reason for the rapid growth of tumors in the V-PBS group. HSPs may be useful therapeutic targets in future research, providing important reference values for the study of avian leukemia and cancer.

As a non-receptor tyrosine kinase, the *v-fps* encoding Gag-fps oncoprotein in acute tumorigenic ALV-J can bind and phosphorylate host cell proteins, activate downstream signaling pathways, and ultimately cause cell transformation and cancer. Feng et al. confirmed that PI3K-Akt signaling was activated upon ALV-J infection. The activation of PI3K-Akt reduced the autophagy of host cells and facilitated the replication and subsequent release of viruses (Feng et al., 2011). It has been reported that ALV-J infection can inhibit the host's antiviral immune response by regulating JAK-STAT signaling, thereby facilitating ALV-J immune escape (Feng et al., 2019). Lan et al. (2017) reported that host's response to ALV-J infection included the identification and defense of pathogens, as well as the activation of apoptotic and inflammatory pathways, p53, RIG-I, STAT3, and NF-κB signaling pathways. *Laminaria japonica* polysaccharides can inhibit IGF-IR and PI3K-Akt signaling pathways in gastric cancer cells (Kwon and Nam, 2007). At the same time, polysaccharides can enhance the immune system by regulating NF-κB. Furthermore, estrogen participates in innate and adaptive immune responses, and it can affect cytokine production. It also has immunoregulatory effects in breast cancer, ovarian cancer, and lung cancer (Hamilton et al., 2016). TPPPS is involved in the regulation of signaling pathways such as P13K-Akt signaling, Ras signaling, JAK-STAT signaling, NF-κB signaling, and estrogen signaling (Table 4). TPPPS may inhibit the replication of Fu-J (SDAU1005) and tumor growth by regulating these signaling pathways.

In conclusion, our results showed that TPPPS could significantly inhibit the replication of the Fu-J virus, as well as its helper virus SDAU1005 *in vivo* and *in vitro*. Transcriptional analysis showed that TPPPS could bind to specific receptors, which activated various signaling pathways to regulate innate and acquired immunity. In addition, TPPPS up-regulated various antiviral and antitumor genes involved in viral replication and tumor inhibition, while down-regulating tumor-causing genes. Although our data is not sufficient to reliably assess correlations between DEGs, RNA-Seq technology may provide new insights on the pathogenesis of ALV-J and the antiviral and antitumor mechanisms of TPPPS. In summary, TPPPS is a compound with antiviral and antitumor properties. Further studies are needed to better understand its benefits.

Declaration of Competing Interest

The authors declare that there is no conflict of interest.

Acknowledgments

This project was supported by National Natural Science Foundation of China (< GN1 > 3177130834), the N < /GN1 > ational Key Research and Development Program of China (2017YFD0500706), and the Funds of Shandong "Double Tops" Program (< GN3 > SYL2017YSTD11) < / GN3 > .

Appendix A. Supplementary data

Supplementary material related to this article can be found, in the online version, at doi:https://doi.org/10.1016/j.vetmic.2019.07.028.

References

Bergqvist, C., Kadara, H., Hamie, L., Nemer, G., Safi, R., Karouni, M., Marrouche, N., Abbas, O., Hasbani, D.J., Kibbi, A.G., Nassar, D., Shimomura, Y., Kurban, M., 2018. SLURP-1 is mutated in Mal de Meleda, a potential molecular signature for melanoma and a putative squamous lineage tumor suppressor gene. Int. J. Dermatol. 57, 162–170.

Chavarria-Velazquez, C.O., Torres-Martinez, A.C., Montano, L.F., Rendon-Huerta, E.P., 2018. TLR2 activation induced by H. Pylori LPS promotes the differential expression of claudin-4, -6, -7 and -9 via either STAT3 and ERK1/2 in AGS cells. Immunobiology 223, 38–48.

Chen, Y., Yao, F., Ming, K., Wang, D., Hu, Y., Liu, J., 2016. Polysaccharides from traditional chinese medicines: extraction, purification, modification, and biological activity. Molecules 21.

Cheng, Z., Liu, J., Cui, Z., Zhang, L., 2010. Tumors associated with avian leukosis virus subgroup J in layer hens during 2007 to 2009 in China. J. Vet. Med. Sci. 72, 1027–1033.

Coy, S., Dubuc, A.M., Dahiya, S., Ligon, K.L., Vasiljevic, A., Santagata, S., 2017. Nuclear CRX and FOXJ1 expression differentiates non-germ cell pineal region tumors and supports the ependymal differentiation of papillary tumor of the pineal region. Am. J. Surg. Pathol. 41, 1410–1421.

Dang, S.S., Jia, X.L., Song, P., Cheng, Y.A., Zhang, X., Sun, M.Z., Liu, E.Q., 2009. Inhibitory effect of emodin and Astragalus polysaccharide on the replication of HBV. World J. Gastroenterol. 15, 5669–5673.

De Marco, M., Basile, A., Iorio, V., Festa, M., Falco, A., Ranieri, B., Pascale, M., Sala, G., Remondelli, P., Capunzo, M., Firpo, M.A., Pezzilli, R., Marzullo, L., Cavallo, P., De Laurenzi, V., Turco, M.C., Rosati, A., 2018. Role of BAG3 in cancer progression: a therapeutic opportunity. Semin. Cell Dev. Biol. 78, 85–92.

Feng, M., Xie, T., Li, Y., Zhang, N., Lu, Q., Zhou, Y., Shi, M., Sun, J., Zhang, X., 2019. A balanced game: chicken macrophage response to ALV-J infection. Vet. Res. 50, 20.

Feng, S.Z., Cao, W.S., Liao, M., 2011. The PI3K/Akt pathway is involved in early infection of some exogenous avian leukosis viruses. J. Gen. Virol. 92, 1688–1697.

Gao, Y.L., Qin, L.T., Pan, W., Wang, Y.Q., Le Qi, X., Gao, H.L., Wang, X.M., 2010. Avian leukosis virus subgroup J in layer chickens. China. Emerg Infect Dis 16, 1637–1638.

Hamilton, D.H., Griner, L.M., Keller, J.M., Hu, X., Southall, N., Marugan, J., David, J.M., Ferrer, M., Palena, C., 2016. Targeting estrogen receptor signaling with fulvestrant enhances immune and chemotherapy-mediated cytotoxicity of human lung Cancer. Clin. Cancer Res. 22, 6204–6216.

Huik, K., Avi, R., Pauskar, M., Kallas, E., Jogeda, E.L., Karki, T., Marsh, K., Des Jarlais, D., Uuskula, A., Lutsar, I., 2013. Association between TLR3 rs3775291 and resistance to HIV among highly exposed Caucasian intravenous drug users. Infect. Genet. Evol. 20, 78–82.

Jhaveri, K., Taldone, T., Modi, S., Chiosis, G., 2012. Advances in the clinical development of heat shock protein 90 (Hsp90) inhibitors in cancers. Biochim. Biophys. Acta 1823, 742–755.

Jiao, S., Li, N., Cai, S., Guo, H., Wen, Y., 2017. Inhibition of CYFIP2 promotes gastric cancer cell proliferation and chemoresistance to 5-fluorouracil through activation of the Akt signaling pathway. Oncol. Lett. 13, 2133–2140.

Justice, J., Malhotra, S., Ruano, M., Li, Y., Zavala, G., Lee, N., Morgan, R., Beemon, K., 2015. The MET gene is a common integration target in avian leukosis virus subgroup J-induced chicken hemangiomas. J. Virol. 89, 4712–4719.

Kouakou, K., Schepetkin, I.A., Yapi, A., Kirpotina, L.N., Jutila, M.A., Quinn, M.T., 2013. Immunomodulatory activity of polysaccharides isolated from Alchornea cordifolia. J. Ethnopharmacol. 146, 232–242.

Kwon, M.J., Nam, T.J., 2007. A polysaccharide of the marine alga Capsosiphon fulvescens induces apoptosis in AGS gastric cancer cells via an IGF-IR-mediated PI3K/Akt pathway. Cell Biol. Int. 31, 768–775.

Lan, X., Wang, Y., Tian, K., Ye, F., Yin, H., Zhao, X., Xu, H., Huang, Y., Liu, H., Hsieh, J.C., Lamont, S.J., Zhu, Q., 2017. Integrated host and viral transcriptome analyses reveal pathology and inflammatory response mechanisms to ALV-J injection in SPF chickens. Sci. Rep. 7, 46156.

Li, B., Wei, K., Yang, S., Yang, Y., Zhang, Y., Zhu, F., Wang, D., Zhu, R., 2015. Immunomodulatory effects of Taishan Pinus massoniana pollen polysaccharide and propolis on immunosuppressed chickens. Microb. Pathog. 78, 7–13.

Li, Z., Li, L., Zhou, H., Zeng, L., Chen, T., Chen, Q., Zhou, B., Wang, Y., Chen, Q., Hu, P., Yang, Z., 2017. Radix isatidis polysaccharides inhibit influenza A virus and influenza A virus-induced inflammation via suppression of host TLR3 signaling in vitro. Molecules 22.

Liu, W., Rodgers, G.P., 2016. Olfactomedin 4 expression and functions in innate immunity, inflammation, and cancer. Cancer Metastasis Rev. 35, 201–212.

Meeusen, B., Janssens, V., 2018. Tumor suppressive protein phosphatases in human cancer: emerging targets for therapeutic intervention and tumor stratification. Int. J. Biochem. Cell Biol. 96, 98–134.

Meng, F., Zhang, W., Wang, Y., 2017. RASAL1 inhibits HepG2 cell growth via HIF-2alpha mediated gluconeogenesis. Oncol. Lett. 14, 7344–7352.

Meng, X., Liang, H., Luo, L., 2016. Antitumor polysaccharides from mushrooms: a review on the structural characteristics, antitumor mechanisms and immunomodulating activities. Carbohydr. Res. 424, 30–41.

Monteiro, M., Evaristo, C., Legrand, A., Nicoletti, A., Rocha, B., 2007. Cartography of gene expression in CD8 single cells: novel CCR7- subsets suggest differentiation independent of CD45RA expression. Blood 109, 2863–2870.

Payne, L.N., Nair, V., 2012. The long view: 40 years of avian leukosis research. Avian Pathol. 41, 11–19.

Plachy, J., Reinisova, M., Kucerova, D., Senigl, F., Stepanets, V., Hron, T., Trejbalova, K., Elleder, D., Hejnar, J., 2017. Identification of new world quails susceptible to infection with avian leukosis virus subgroup. J. J Virol 91.

Rohr, J., Guo, S., Huo, J., Bouska, A., Lachel, C., Li, Y., Simone, P.D., Zhang, W., Gong, Q., Wang, C., Cannon, A., Heavican, T., Mottok, A., Hung, S., Rosenwald, A., Gascoyne, R., Fu, K., Greiner, T.C., Weisenburger, D.D., Vose, J.M., Staudt, L.M., Xiao, W., Borgstahl, G.E., Davis, S., Steidl, C., McKeithan, T., Iqbal, J., Chan, W.C., 2016. Recurrent activating mutations of CD28 in peripheral T-cell lymphomas. Leukemia 30, 1062–1070.

Sheng, X., Bowen, N., Wang, Z., 2016. GLI pathogenesis-related 1 functions as a tumor-suppressor in lung cancer. Mol. Cancer 15, 25.

Wang, X., Xue, Y., Li, Y., Liu, F., Yan, Y., Zhang, H., Jin, Q., 2018. Effects of Isatis root polysaccharide in mice infected with H3N2 swine influenza virus. Res. Vet. Sci. 119, 91–98.

Wang, Y., Li, J., Li, Y., Fang, L., Sun, X., Chang, S., Zhao, P., Cui, Z., 2016. Identification of ALV-J associated acutely transforming virus Fu-J carrying complete v-fps oncogene. Virus Genes 52, 365–371.

Yang, S., Wei, K., Jia, F., Zhao, X., Cui, G., Guo, F., Zhu, R., 2015. Characterization and biological activity of Taishan Pinus massoniana pollen polysaccharide in vitro. PLoS One 10, e0115638.

Yu, C., Wei, K., Liu, L., Yang, S., Hu, L., Zhao, P., Meng, X., Shao, M., Wang, C., Zhu, L., Zhang, H., Li, Y., Zhu, R., 2017. Taishan Pinus massoniana pollen polysaccharide inhibits subgroup J avian leucosis virus infection by directly blocking virus infection and improving immunity. Sci. Rep. 7, 44353.

Zhou, L., Liu, Z., Wang, Z., Yu, S., Long, T., Zhou, X., Bao, Y., 2017. Astragalus polysaccharides exerts immunomodulatory effects via TLR4-mediated MyD88-dependent signaling pathway in vitro and in vivo. Sci. Rep. 7, 44822.